Differentiation (2007) 75:978–991 DOI: 10.1111/j.1432-0436.2007.00182.x Journal compilation © 2007, International Society of Differentiation

ORIGINAL ARTICLE

Mary Ramsey · Christina Shoemaker · David Crews

Gonadal expression of *Sf1* and aromatase during sex determination in the red-eared slider turtle (*Trachemys scripta*), a reptile with temperature-dependent sex determination

Received November 6, 2006; accepted in revised form March 5, 2007

Abstract Many egg-laying reptiles have temperature-dependent sex determination (TSD), where the offspring sex is determined by incubation temperature during a temperature-sensitive period (TSP) in the middle third of development. The underlying mechanism transducing a temperature cue into an ovary or testis is unknown, but it is known that steroid hormones play an important role. During the TSP, exogenous application of estrogen can override a temperature cue and produce females, while blocking the activity of aromatase (*Cyp19a1*), the enzyme that converts testosterone to estradiol, produces males from a female-biased temperature. The production of estrogen is a key step in ovarian differentiation for many vertebrates, including TSD reptiles, and temperature-based differences in aromatase expression during the TSP may be a critical step in ovarian determination. Steroidogenic factor-1 (*Sf1*) is a key gene in vertebrate sex determination and regulates many steroidogenic enzymes, including aromatase. We find that *Sf1* and aromatase are differentially expressed during sex determination in the red-eared slider turtle, *Trachemys scripta elegans*. *Sf1* is expressed at higher levels during testis development while aromatase expression increases during ovary determination. We also assayed *Sf1* and aromatase response to sex-reversing treatments via temperature or the modulation of estrogen availability. *Sf1* expression was redirected to low-level female-specific patterns with feminizing temperature shift or exogenous estradiol application and redirected to more intense male-specific patterns with male-producing temperature shift or inhibition of aromatase activity. Conversely, aromatase expression was redirected to more intense female-specific patterns with female-producing treatment and redirected toward diffuse low-level male-specific patterns with masculinizing sex reversal. Our data do not lend support to a role for *Sf1* in the regulation of aromatase expression during slider turtle sex determination, but do support a critical role for estrogen in ovarian development.

Key words temperature-dependent sex determination · reptile · steroidogenesis · differentiation · ovary · aromatase · *Sf1*

Mary Ramsey · Christina Shoemaker · David Crews (✉)
Department of Integrative Biology
University of Texas, Austin, TX, U.S.A.
Tel: +1 512 471 1113
Fax: +1 512 471 6078
E-mail: crews@mail.utexas.edu

Introduction

Two primary forms of sex determination exist among vertebrates. In genotypic sex determination (GSD), a genetic factor such as the *Sry* gene found on the mammalian Y chromosome determines sex. In environmental sex determination, environmental cues dictate sex determination. One form of environmental sex determination found in many egg-laying reptiles is temperature-dependent sex determination (TSD). In the red-eared slider turtle (*Trachemys scripta elegans*), gonadal sex is determined by incubation temperature during a temperature-sensitive period (TSP) spanning about the middle third of development (Wibbels et al., 1991a). The TSP and the ensuing phase of gonadal differentiation can be further divided into three phases: bipotential gonad (Stages 14–15, when the gonad is morphologically bipotential although temperature may already be exerting its action), sex determination (Stages 16–19, when the sexual trajectory of the gonadal primordium is still flexible), and gonadal commitment/differentiation (Stages 20 to hatch, when the final gonadal morphology develops and sex is irreversible). During

the TSP, warmer temperatures (31°C) produce 100% female hatchlings and cooler temperatures (26°C) produce 100% males, while intermediate temperatures produce mixed sex ratios. For example, an incubation temperature of 29.4°C results in an 80:20 female-biased sex ratio. Sex determination is labile throughout the TSP, and shifting embryos from 31°C to 26°C or 26°C to 31°C reverses sex outcome (Wibbels et al., 1991a).

While the actual triggering mechanisms that initiate a sex-determining gene cascade are diverse, many aspects of sex determination, and more particularly, gonadal differentiation, are remarkably conserved across vertebrate groups. Genes implicated in mammalian sex determination and gonadal differentiation such as *Sox9*, *Dmrt1*, *Mis*, *Sf1*, *Wnt4*, *Dax1*, and *FoxL2* have also been found in avian and reptile species, including reptiles with TSD (Spotila et al., 1998; Fleming et al., 1999; Western et al., 1999, 2000; Smith et al., 1999b; Kettlewell et al., 2000; Maldonado et al., 2002; Loffler et al., 2003; Murdock and Wibbels, 2003b; Govoroun et al., 2004).

Another conserved feature of vertebrate sex determination is the ability of steroid hormones to influence either GSD (except in eutherian mammals) or TSD. In many vertebrates, estrogen plays a prominent role in the differentiation of ovaries. Application of estrogen during the period of sexual differentiation will induce partial to complete sex reversal in marsupials (Coveney et al., 2001), transient feminization in birds (Scheib, 1983), and permanent sex reversal in fish (Baroiller et al., 1999), amphibians (Wallace et al., 1999), and reptiles (Bull et al., 1988). In the slider turtle, application of estrogen to the egg during the TSP overrides a male-determining temperature cue and produces all female hatchlings that are morphologically indistinguishable from females produced via warmer female-determining temperatures (Wibbels et al., 1993). Similarly, inhibition of Cyp19a1 (hereafter referred to as aromatase), the enzyme that converts testosterone to estradiol (E_2), during the TSP produces male hatchlings from female-biased temperatures (Crews and Bergeron, 1994; Crews et al., 1994). This effect is also conserved. For example, inhibiting aromatase early in development permanently sex reverses genetically female chickens (Elbrecht and Smith, 1992) and creates males from an all-female parthenogenic lizard species (Wibbels and Crews, 1994; Wennstrom and Crews, 1995).

Because estrogens and aromatase inhibitors (AIs) can override a temperature cue for sex determination in TSD reptiles, it has been hypothesized that temperature-based changes in estrogen levels are a critical step for ovarian development (Crews et al., 1994; Pieau and Dorizzi, 2004). If temperature and estrogen action are intimately linked in TSD, then examining aromatase expression in the gonad becomes critical to understanding the complex interplay between temperature, steroid hormones, and other sex-determining genes that underlie sex determination in a TSD reptile. Of particular interest in this context is steroidogenic factor-1 (*Sf1*), a gene known to regulate the expression of gonadal steroidogenic enzymes including aromatase (Morohashi and Omura, 1996; Parker et al., 2002). *Sf1* is critical in vertebrate sex determination and differentiation regardless of sex-determining mechanism. Beyond its steroidogenic functions, Sf1 is required for maintenance of the early bipotential gonad and plays a critical role in testis differentiation. *Sf1* mRNA is expressed at higher levels in developing mammalian testes (Ikeda et al., 1994), a pattern conserved in the slider turtle (Fleming et al., 1999). *Sf1* is also responsive to sex-reversing treatments: *Sf1* levels increase with a male-producing temperature shift and AI treatment and will decrease with the corresponding female-producing shift and exogenous estrogen application (Fleming and Crews, 2001).

The current study localizes *Sf1* and aromatase mRNA expression using whole-mount *in situ* hybridization (ISH) at male- and female-producing temperatures from the early bipotential gonad through the TSP and sexual differentiation. We also document changes in *Sf1* and aromatase localization in response to sex-reversing treatment by temperature shifts and application of exogenous estrogen or AI to incubating eggs during the TSP. Finally, quantitative real-time polymerase chain reaction (qPCR) is used to quantify *Sf1* and aromatase mRNA levels in isolated gonad tissue from embryos incubating at male- and female-producing temperatures.

Methods

Tissue collection

Red-eared slider turtle (*T. scripta*) eggs were purchased from Robert Clark (Clark Turtle Farms, Hammond, LA). The eggs were picked up within 24 hr of laying so all embryos in each group/shipment were at roughly equivalent developmental stages. To control for possible clutch effects, collected eggs were randomized on site. Eggs were kept at room temperature (22°C) in Texas until candled to establish viability, at which time they were further randomized and placed into trays (35/tray) containing 1:1 vermiculite and water mix and placed in incubators (Precision, Chicago, IL) at 26°C (male-producing temperature), 29.4°C (female-biased temperature), or 31°C (female-producing temperature). Temperatures within the incubators were monitored continuously with HOBO recording devices (Onset Computer Corporation, Bourne, MA) as well as checked daily using calibrated shelf thermometers. To avoid small temperature gradient effects, the egg trays were rotated daily within the incubator. A few eggs (two to three) were dissected at regular intervals to assess developmental stage (Yntema, 1968). Embryos were harvested at Stages 15, 17, 19, 21, and 23. Adrenal-kidney-gonad (AKG) or isolated gonad tissue was rapidly dissected and processed for experimental use.

In addition to eggs incubated at constant temperatures, eggs were manipulated either by shifting them to a different temperature (Table 1) or by chemical manipulation (Table 2) with all sex-reversing treatments occurring at Stage 17 (midway through the TSP). For the temperature shifts, one group was shifted from 26°C

Table 1 Effect of temperature

Group	Hatch sex ratio*
26°C	0 (65)
31°C	100 (114)
26°C → 31°C	94 (38)
31°C → 26°C	19 (43)

*Given as % female, (# individuals).

to 31°C, with another receiving the complementary shift from 31°C to 26°C. For the hormone treatment, groups incubating at 26°C and 31°C were treated with 5 µg estradiol-17β (Sigma, St. Louis, MO) in 5 µl 95% EtOH, each with control groups receiving EtOH vehicle. Other eggs were incubated at the intermediate temperature of 29.4°C, a temperature that produces a female-biased sex ratio (typically 80:20 female:male, see Table 2). One group was treated with 100 µg of the AI fadrozole (CGS16949A, Ciba-Geigy, Summit, NJ) in 5 µl 95% EtOH with a control group treated with EtOH alone. Treated groups were harvested at Stages 19 and 23 except for estradiol-treated eggs at 31°C, which were harvested at Stage 23 alone. For each treatment, a subset of eggs was allowed to develop through hatching and was sexed by gross morphology of the gonad.

Whole-mount ISH

A 337 bp sub-clone of slider turtle aromatase (Accession AF178949) was cloned into pCR 4-TOPO vector (Invitrogen, Carlsbad, CA) according to the manufacturer's protocol. Turtle *Sf1* (Accession AF033833) cloning and probe length have been reported previously (Fleming et al., 1999). Digoxigenin (DIG)-labeled turtle aromatase and *Sf1* antisense and sense control probes were transcribed using Megascript High Yield Transcription kit (Ambion, Austin, TX) with 33% labeled digoxigenin-11-UTP (Roche, Indianapolis, IN) and 67% unlabeled UTP, following the manufacturer's protocol. Probe integrity and abundance was assessed through gel electrophoresis.

For each gene, whole-mount ISH experiments were conducted on AKG tissue from four embryos/stage/treatment ($N = 88$ embryos/gene). The ISH experiments were conducted as described (Smith et al., 1999a) but modified for use with turtle tissue. Briefly, AKG tissue was fixed overnight in 4% paraformaldehyde (PFA) and then sequentially dehydrated with MeOH:PBTX solutions, ending in 100% MeOH for storage at −20°C. ISH was performed using hybridization solution containing 4–8 µl of DIG-labeled antisense probe. Samples were incubated overnight (4°C) with anti-digoxigenin-AP antibody (Roche) preabsorbed with embryo powder derived from whole body and AKG embryonic turtle tissue. Basement membrane (BM) purple AP substrate (Roche) was used for colorimetric detection. For each gene, color detection for all groups in a given stage was halted simultaneously. Color detection times were optimized for each gene/developmental stage and ranged from 5 to 8 hr. Detection times were as follows: St 15 SF1 5.5 hr, Aromatase 8 hr; St 17 SF1 7 hr, Aromatase 7.5 hr, St 19 SF1 7 hr, Aromatase 7 hr, St 23 SF1 8 hr, Aromatase 8.5 hr. To view internal gonadal structure/signal, whole-mount tissue was sectioned on a Microm HM 500 OM cryostat (Microm International, Walldorf, Germany) at 25 or 40 µm thickness. No specific signal was detected in embryos hybridized with labeled sense control probe (Fig. 1). All section photographs were taken on a Nikon Eclipse 80i microscope (Nikon Instruments, Melville, NY) using NIS-Elements BR 220 visualization software. LUT settings were 125-black, 255-white, and gamma 0.75 for all photomicrographs except for *Sf1* at Stage 15 which were visualized at 85-black due to intensity of signal. ×100 photomicrographs (Fig. 2) were taken on an Olympus BX61 microscope (Olympus American Inc., Center Valley, PA) using MicroFire S99808 video camera (Optronics, Goleta, CA).

Table 2 Effect of chemical manipulation

Group	Hatch sex ratio*
26°C EtOH	0 (48)
26°C E_2	100 (53)
31°C EtOH	100 (25)
31°C E_2	100 (30)
29.4°C EtOH	82 (83)
29.4°C AI	12 (68)

*Given as % female, (# individuals).
E_2, estradiol; AI, aromatase inhibitor.

Total RNA preparation and cDNA synthesis

Aromatase and *Sf1* are expressed in the surrounding kidney and adrenal compartments of the AKG complex as well as the gonad at both incubation temperatures (White and Thomas, 1992; Fleming et al., 1999). To isolate temperature-specific differences in expression levels within the gonad itself, gonads were excised from surrounding tissue for analysis. Because the gonad is a very small component of the AKG, gonads from multiple individuals (30–50/sample) were pooled for measurement.

Gonads were rapidly dissected away from the adjacent adrenal/kidney tissue and placed in RNAlater (Ambion) for overnight incubation at 4°C followed by storage at −80°C, or placed directly into Promega RNAgents Total RNA Isolation kit (Promega, Madison, WI) denaturing solution and stored at −80°C. Total RNA was then extracted from the gonad tissue using RNAgents Total RNA Isolation kit (Promega) following the manufacturer's protocol. Total RNA abundance and purity was assessed through spectophotometry readings at 260 and 280 nm.

Before cDNA synthesis, total RNA was treated with DNase to ensure elimination of genomic DNA contamination using the Turbo DNA-Free kit (Ambion) following the manufacturer's protocol. Single-stranded cDNA was then reverse-transcribed at a concentration of 1 µg total RNA/20 µl synthesis reaction using Superscript First Strand Synthesis for RT-PCR kit (Invitrogen). cDNA synthesis was primed with both oligo-dT and random hexamers using a modified manufacturer's protocol (Invitrogen).

Real-time qPCR

Real-time PCR quantification results are typically normalized to a housekeeping gene, but many housekeeping genes previously considered to be constitutively expressed were found to be regulated by particular treatments, tissue types, or developmental stage (Pfaffl, 2001; Bustin, 2002). Therefore, to select an appropriate normalizing gene, five candidate slider turtle housekeeping genes (Table 3) plus slider turtle 16S rRNA sequence were tested on cDNA template derived from AKG total RNA for all stages and treatments used in these experiments. GeNORM (http://medgen.ugent.be/~jvdesomp/genorm/; Vandesompele et al., 2002) program was used to assess the most stably expressed genes. Protein phosphatase 1 γ (PP1) was chosen based on stability of expression under experimental conditions and relative level of abundance compared with aromatase and *Sf1* transcript levels.

Real-time PCR primer sequences and amplicon size are described below (Table 4). Aromatase primers were designed using LUX primer design program (www.invitrogen.com/LUX) and *Sf1* and PP1 primers were designed using MacVector (Accelrys Inc., San Diego, CA) software program. All primers were engineered to cross exon boundaries (estimated from human gene structure) to eliminate possible signal contamination from genomic DNA. Specificity of target was verified by gel electrophoresis.

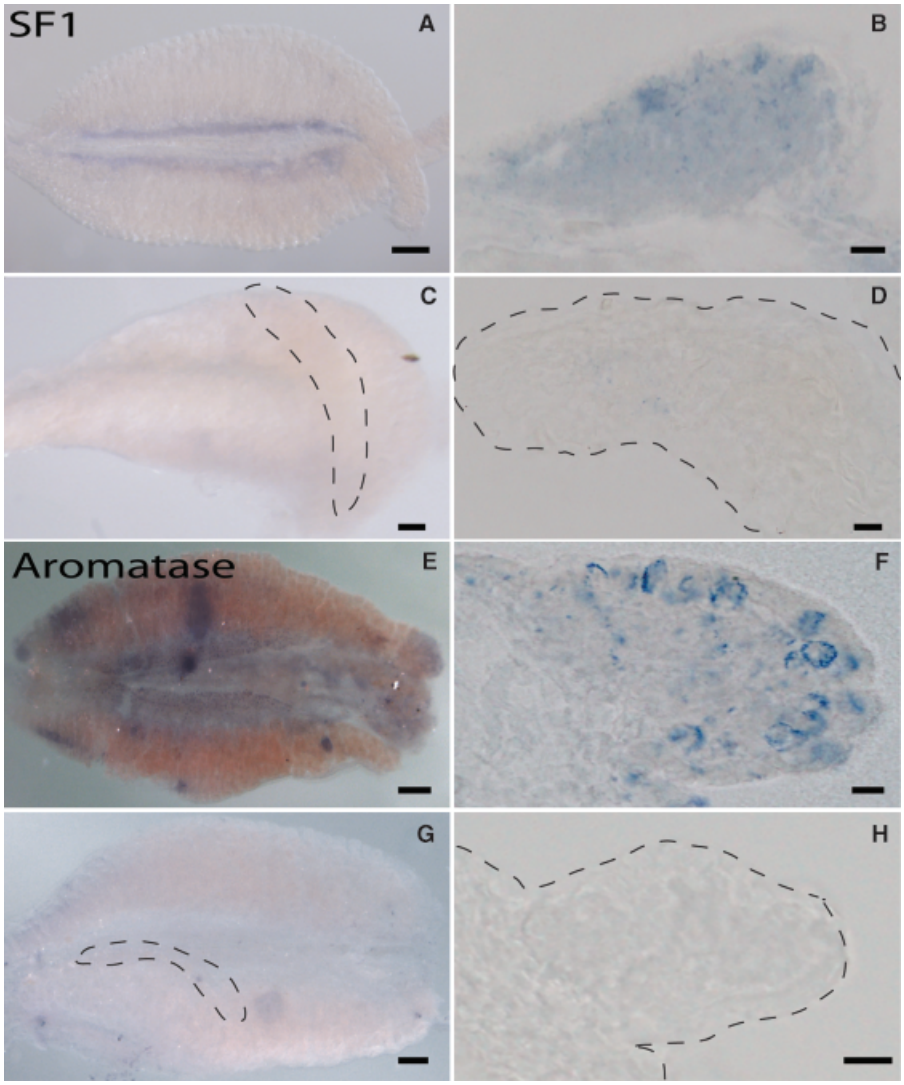

Fig. 1 Steroidogenic factor-1 (SF1) and aromatase whole-mount *in situ* hybridization (ISH) expression and probe specificity. SF1 and aromatase are expressed along the gonad in a whole-mount adrenal-kidney-gonad (AKG) (**A**, **E**) but not in Digoxigenin (DIG)-labeled sense controls (**C**, **G**). Adjacent to each whole mount, a photomicrograph of a representative section from the pictured AKG show specific signal in gonads hybridized with DIG-labeled antisense probe (**B**, **F**) but not sense controls (**D**, **H**). Dashed lines outline sense-hybridized gonads (C, D; G, H). Pictured gonads were incubated at the female-producing temperature (FPT; 31°C) and were dissected at Stage 17 (midway through the temperature-sensitive period [TSP]). Whole-mount gonads were sectioned at 40 µm thickness. Scale bar = 10 µm in (B, D, F, H) and 250 µm in (A, C, E, G).

Real-time qPCR experiments were conducted on ABI Prism 7900 real-time PCR machine (Applied Biosystems, Foster City, CA). cDNA representing 10 ng starting total RNA was used in a 10 µl reaction containing 2 µl cDNA template, 5 µl 2 × Platinum SYBR Green qPCR SuperMix UDG (Invitrogen), and 5 pmol aromatase or *Sf1* primers or 3 pmol PP1 primers. Real-time qPCR parameters were 2 min at 50°C, 2 min at 95°C for denaturing, followed by 40 cycles at 15 sec 95°C, 15 sec 60°C, and 15 sec 72°C. Each gene primer pair showed no signal in no-template and no-RT controls. Relative gene expression levels were assessed using SYBR green detection chemistry. Dissociation curve analysis was performed after each assay to determine target specificity. Each sample was run in triplicate.

Real-time qPCR data analysis

Real-time qPCR run results were first analyzed using the Applied Biosystems Sequence Detection System software (SDS 2.2.1). Relative quantification was performed by a modified comparative critical threshold (CT) method that corrects for different PCR amplification efficiencies among primer pairs (Simon, 2003). Gene expression normalized to PP1 housekeeping is given as mean normalized expression (MNE) = $(E_{\mathrm{pp1}}^{\mathrm{meanCT_{pp1}}})/(E_{\mathrm{arom\,or\,}Sf1}^{\mathrm{meanCT_{arom\,or\,}Sf1}})$, where E is the PCR efficiency ($E = 10^{-(1/\mathrm{slope})}$) (Pfaffl, 2001) and meanCT is the average CT across the three replicates.

Results

Developmental analysis of *Sf1* expression

Sf1 is present in the gonad throughout all three phases of gonadal development. High levels of *Sf1* are expressed at both male- and female-producing temperatures at the onset of the TSP (Stage 15; Figs. 2A,2G). As the gonad enters the sex-determining stages of development (Stage 17), *Sf1* expression begins to dissipate at the female-producing temperature, but at the male-producing temperature is localized to the presumptive supporting cell lineage surrounding germ cells located predominately in the cortex at this stage of development (Figs. 2B,2H,3A,3B). At Stage 19, *Sf1* expression remains diffuse throughout the medullary region in the

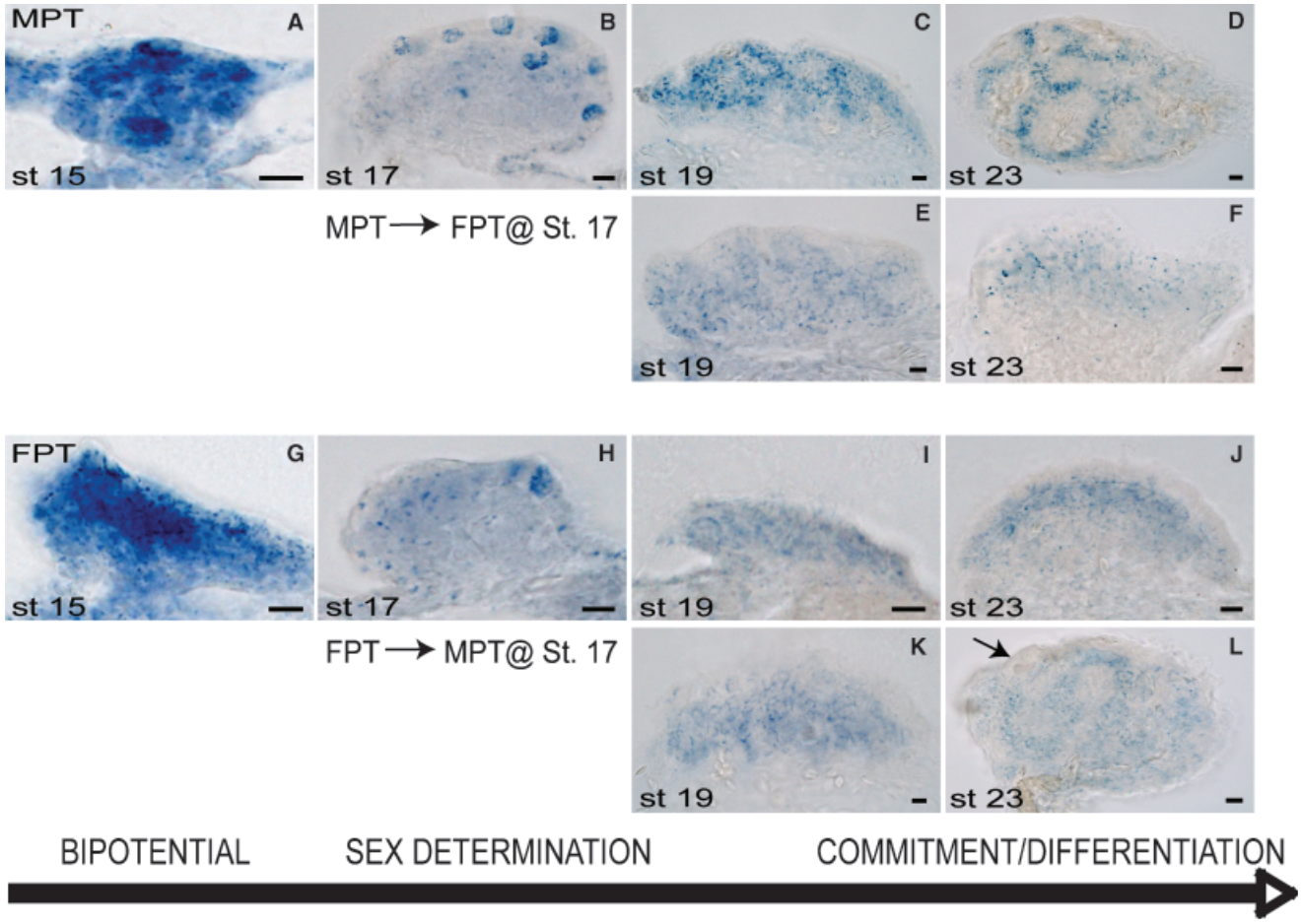

Fig. 2 Steroidogenic factor-1 (*Sf1*) expression in the gonad changes over time and is altered following a sex-reversing temperature shift. *Sf1* localization patterns differ by sex when analyzed at male-producing temperature (**A–D**) and female producing temperature (**G–J**) throughout the temperature-sensitive period (TSP). Embryos were shifted between incubation temperatures midway through the TSP (Stage 17). *Sf1* expression patterns are temperature-sensitive and show changes two and four stages after temperature shift from male- to female-producing temperatures (**E**, **F**) and vice versa (**K**, **L**). MPT, male-producing temperature (26°C); FPT, female-producing temperature (31°C). MPT → FPT shift = 26°C → 31°C. FPT → MPT shift = 31°C → 26°C. Arrow indicates cortical remnants in the temperature-shifted testis (L). Whole-mount gonads were sectioned at 40 μm thickness. Scale bar = 10 μm.

developing ovary, while expression is more prominent at the male-producing temperature, and localizes to the developing sex cords (Figs. 2C,2I). At Stage 23, when gonadal differentiation is well underway and sex outcome is irreversible, expression at the female-producing temperature continues to show scattered medullary expression as well as localization along the medullary/cortical boundary, while strong medullary striping is evident in the developing testis (Figs. 2D,2J).

Developmental analysis of aromatase expression

Aromatase is present throughout the TSP at both male- and female-producing incubation temperatures, but localization patterns differ both according to incubation temperature and embryonic state (Fig. 4). At the female-producing temperature, aromatase is localized to presumptive supporting cells surrounding germ cells in the bipotential genital ridge at the onset of the TSP (Stage 15). This female-specific localization pattern precedes organization at the male-producing temperature (Figs. 4A,4G).

By the middle of the TSP (Stage 17), the gonad is still bipotential but temperature-based gene expression patterns are already beginning to direct the gonad along a developmental trajectory toward an ovary or a testis (Crews et al., 2006). At this stage, aromatase expression appears equivalent between the two temperatures, but the tendency toward higher levels of organization in the supporting cell lineage around germ cells at the female-producing temperature remains (Figs. 3C,3D,4B,4H). Importantly, this difference in organization is occurring at a developmental stage not only during the TSP, but also while aromatase abundance in the gonad itself is not markedly different between sexes (Fig. 5B).

Table 3 Housekeeping gene candidates and homology to *Mus musculus*

Gene	Clone length	Homology	Accession number
Beta actin	396	86	DQ848990
16S rRNA	323	N/A	AB090050
UBED2	321	93	DQ848992
PP1	479	79	DQ848991
HPRT1	312	81	DQ848993
ALAS1	550	78	DQ848994

At Stage 19, as the TSP closes at the female-producing temperature, the peri-germ cell localization pattern of aromatase persists at the female-producing temperature, and also includes some specific expression along the presumptive medullary–cortical boundary as well as increasing medullary expression. At the male-producing temperature, sex determination is still somewhat labile, but aromatase expression is beginning to organize into a striping pattern in the medullary compartment, reflecting the onset of testis differentiation and a transition away from bipotentiality (Figs. 4C,4I).

During ovarian differentiation (Stage 23), aromatase expression is faint but some expression can be seen localized around the regressing medullary cords and at the cortical/medullary boundary. In the differentiating testis, localization of aromatase around nascent seminiferous tubules diminishes until it is barely perceptible at Stage 23 (Figs. 4D,4J).

Real-time qPCR during development in isolated gonad tissue

Sf1 and aromatase transcript abundance was measured using qPCR. *Sf1* gonadal qPCR expression is higher at the male-producing temperature than the female-producing temperature across development (Fig. 5A). Aromatase abundance measured from isolated gonad tissue shows higher levels of expression at the female-producing temperature from late in the TSP (Stage 19) through ovarian differentiation (Stages 21/23) (Fig. 5B), although differences between the two temperatures do not become pronounced until later in development.

When maximum levels of expression between the two temperatures are compared (Fig. 5C), aromatase levels at the onset of the sex-determining period (Stage 17) are at their highest for an embryo incubating at a male-producing temperature (and will consequently drop and then plateau) and at their lowest for putative females. The lack of correlation between *Sf1* and aromatase abundance patterns is highlighted by examining the relationship between each gene's percent maximum expression across temperatures (Fig. 5D). The ratio of *Sf1*/aromatase shows that *Sf1* is expressed at high levels at male-producing temperature when aromatase expression is low, while aromatase is highly expressed at female-producing temperatures when *Sf1* expression is low.

Changes in *Sf1* and aromatase expression patterns following sex reversal treatments temperature shifts

Patterns of gene expression are altered when eggs are shifted at Stage 17 from male- to female-producing temperatures (M → F) or female- to male-producing temperatures (F → M). *Sf1* and aromatase expression patterns were analyzed following both shifts at Stages 19 (during sex determination) and 23 (during gonadal commitment/differentiation). In the M → F shift, *Sf1* expression begins to lose the male-typical, intense medullary organization by Stage 19 (Figs. 2C,2E), and by Stage 23, the differentiating ovary exhibits the female-typical, diffuse medullary signal (Figs. 2D,2F). In the F → M shift, the gonad shows incipient male-typical *Sf1* expression along developing seminiferous tubules by Stage 19 (Figs. 2I,2K), indicating the gonad has already begun to reset the developmental trajectory toward testis formation. By Stage 23, male-specific *Sf1* expression along the seminiferous tubules is evident, although some cortical development remains (Figs. 2J,2L).

At Stage 19, two stages after the M → F shift, aromatase expression increased in organization compared with the unshifted control (Figs. 4C,4E), with female-typical expression patterns evident by Stage 23 (Figs. 4D,4F). Following the opposing F → M shift, aromatase expression is redirected away from female-specific organization by Stage 19 (Figs. 4I,4K), although the

Table 4 Real-time qPCR primer sequences

Gene	Amplicon (bp)	Primer sequence
SF1	103	For 5′-GGTGGATCGACAAGAGTTTGTGTG-3′ Rev 5′-TTTCTCCTGAGCATCCTTCGCC-3′
Aromatase	95	For 5′-GCACATGGACTTTGCATCACA-3′ Rev 5′-GAACCATCATCTCCAACACACACTGGTTC-3′
PP1	95	For 5′-CAGCAGACCCTGAGAACTTCTTCCTG-3′ Rev 5′-GCGCCTCTTGCACTCATCAT-3′

PCR, polymerase chain reaction.

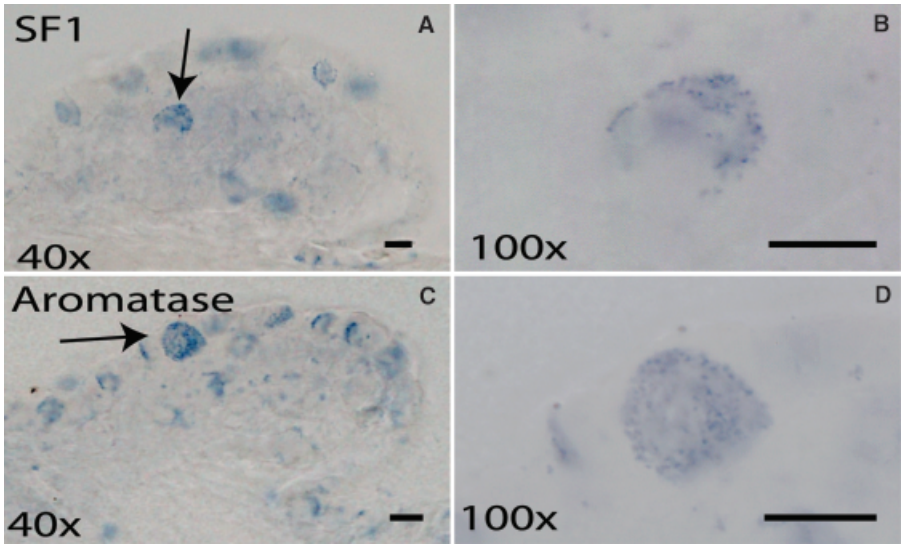

Fig. 3 Higher magnification views of Steroidogenic factor-1 (SF1) and aromatase expression during the TSP. Photomicrographs show SF1 and aromatase localization at ×40 and ×100 magnification. Although the gonad is bipotential at this stage of development (Stage 17, midway through the TSP), gene expression patterns are already becoming sexually dimorphic. SF1 (**A**, **B**) at MPT and Aromatase (**C**, **D**) at FPT form ring-like structures around putative germ cells in the bipotential gonad. Arrows in (A, C) point to structure magnified in (B, D). TSP, temperature-sensitive period; MPT, male-producing temperature (26°C); FPT, female-producing temperature (31°C). Whole-mount gonads were sectioned at 40 μm thickness. Scale bar = 10 μm.

gonad still shows morphological signs of ovarian-specific cortical development. By Stage 23, low-level male-specific aromatase expression patterns predominate in the developing testis, although remnants of the cortical compartment remain (Figs. 4J,4L).

Estradiol treatment at the male-producing temperature

Treatment of eggs at the male-producing incubation temperature with exogenous estradiol-17β (E_2) during the TSP (Stage 17) results in all female hatchlings (Crews et al., 1994). Here, we show that *Sf1* expression levels are less intense following exogenous E_2 treatment (Figs. 6A,6B) and fall to near negligible levels during ovarian differentiation at Stage 23 (Figs. 6C,6D).

In contrast, aromatase expression remains high two stages after estradiol application (Stage 19), and there is a tendency for signal to concentrate around the nascent cortical/medullary boundary and into the developing cortical compartment itself (Figs. 6G,6H). This trend in cortical aromatase localization persists (Figs. 6I,6J) as hormone-induced ovarian differentiation continues (Stage 23), and is more evident in E_2-treated ovaries incubated at the male-producing temperature than untreated ovaries developing at female temperatures (Figs. 4J,6J).

Estradiol treatment at the female-producing temperature

Sf1 and aromatase expression patterns were also examined after application of estradiol to eggs incubating at the female-producing temperature. The feminizing effect of temperature and exogenous estrogen creates a unique phenotype featuring ovaries with enlarged cortical compartments (Figs. 6F,6L). With this treatment, *Sf1* tends to exhibit more intense signal than the typically diffuse pattern exhibited in ovaries created via temperature (Figs. 6E,2F,2J) or via estradiol application at a male-producing temperature (Fig. 6D). Similarly, while light aromatase transcript can be detected in the medullary compartment of all differentiated ovaries, only ovaries receiving both feminizing temperature and estradiol treatment exhibited the intense and organized medullary signal shown here (Figs. 4F,4J,6K,6L,7G).

Treatment with AI at the female-biased incubation temperature

Application of AI during the TSP (Stage 17) causes sex reversal in embryos incubating at an intermediate, female-biased (29.4°C) temperature, thus increasing the percentage of males (Crews and Bergeron, 1994). *Sf1* localization patterns are not altered at Stage 19 following application of AI (Figs. 7A,7B). By Stage 23, however, *Sf1* shows more male-typical expression along the developing seminiferous tubules, while the vehicle-treated ovary exhibits negligible signal with some light expression along the cortical/medullary boundary (Figs. 7C,7D).

AI treatment also does not alter aromatase expression at Stage 19, two embryonic stages after the original application (Figs. 7E,7F). However, as with the masculinizing temperature shift, aromatase localization does shift to a low-level, male-typical pattern as testis morphology becomes evident by Stage 23 (Figs. 7G,7H). EtOH-treated females at the female-biased temperature exhibited similar patterns of expression as untreated 29.4°C controls (data not shown), as well as females incubating at the female-producing temperature (31°) (Figs. 2J,4J).

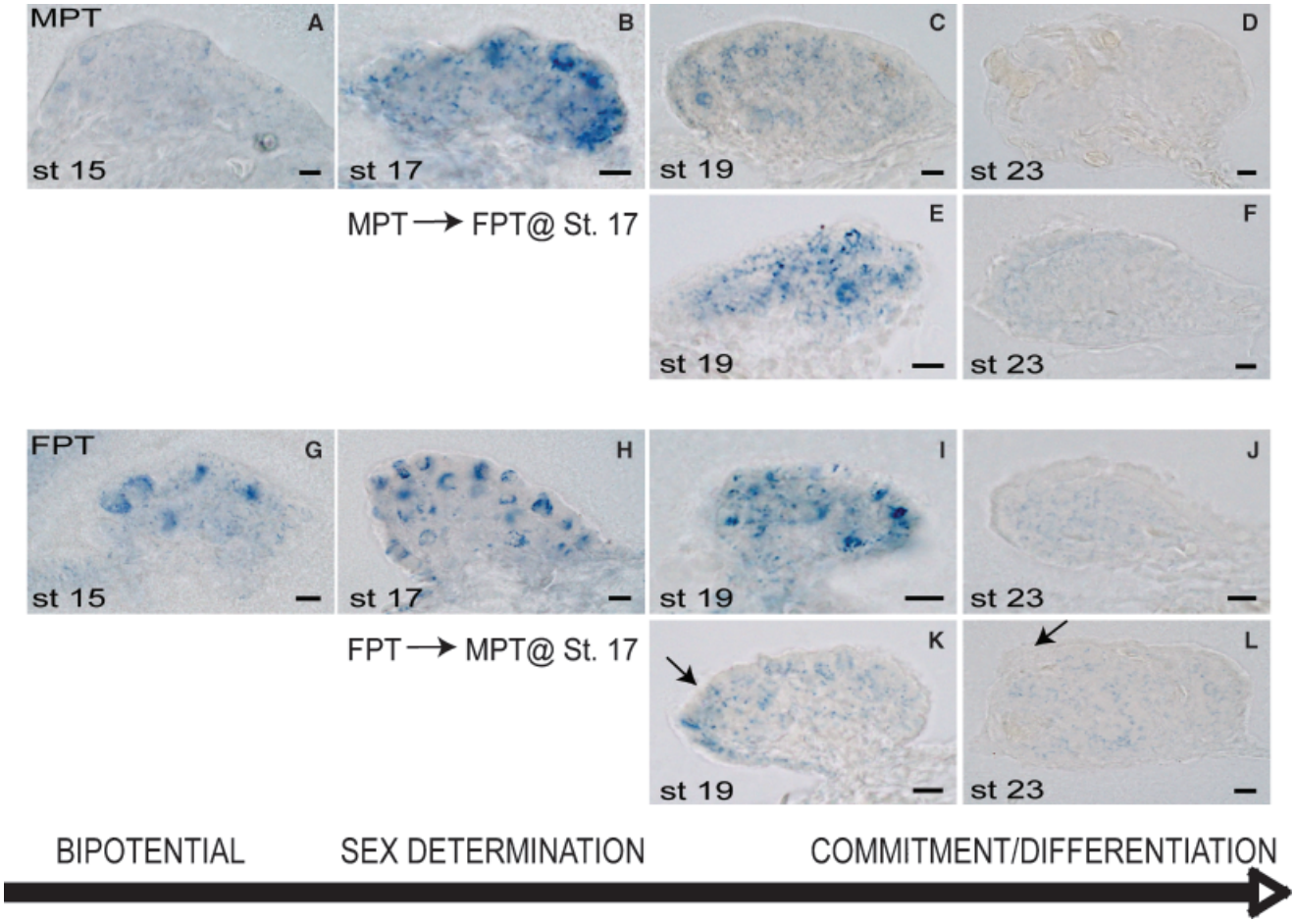

Fig. 4 Aromatase gonadal localization is sexually dimorphic in the bipotential gonad and is altered following a sex-reversing temperature shift. Aromatase localization is differential by sex throughout the three phases of gonadal development. Aromatase expression is more diffuse at male-producing temperatures (**A–D**) and more intensely localized at female-producing temperatures (**G–J**). Aromatase expression patterns are temperature-sensitive and are altered two and four stages after temperature shifts from male- to female-producing temperatures (**E**, **F**) and vice versa (**K**, **L**). MPT, male-producing temperature (26°C); FPT, female-producing temperature (31°C). Arrow indicates cortical remnants in the temperature-shifted testis (C, L). Whole-mount gonads were sectioned at 40 μm thickness (A–C, E, G–I, K) except for Stage 23 gonads (D, F, J, L), which were sectioned at 25 μm thickness. Scale bar = 10 μm.

Discussion

If estrogen is a critical endogenous component in the determination and differentiation of the ovary in the slider turtle, then possible temperature-specific differences in embryonic aromatase expression or activity may be mediating the gonadal steroid hormone milieu. We report an increase in female temperature-specific aromatase expression late in the TSP itself, before sex is committed. Our data suggest a role for differential estrogen production in ovarian determination/differentiation, and supports earlier work on the pond turtle (*Emys orbicularis*), where aromatase activity increased late in the TSP at a female-producing temperature (reviewed in Pieau et al., 1999). This increase in aromatase expression is earlier in gonadal development than observed in previous studies in slider turtle (Willingham et al., 2000; Murdock and Wibbels, 2003a) or alligator (Smith et al., 1995; Gabriel et al., 2001) and is likely due to the inclusion of the kidney and adrenal components of the AKG, the tissue used in these earlier studies. The gonad is a very small fraction of the AKG complex, and kidney and adrenal transcript pools appear to reduce the sensitivity of gonad-specific measurements, as has been suggested by Pieau and Dorizzi (2004). Indeed, when we include the entire AKG complex and measure aromatase expression in our qPCR assay, we also do not pick up a female-specific increase until late in ovarian development (M. Ramsey and D. Crews, unpublished data).

Aromatase expression indicates possible sites of estrogen synthesis in the developing gonad, and *Sf1* expression is examined as a possible indicator of steroidogenic regulation as well as a marker of reversal/commitment to sexual fate. In the differentiating ovary, the requirement for steroidogenesis during

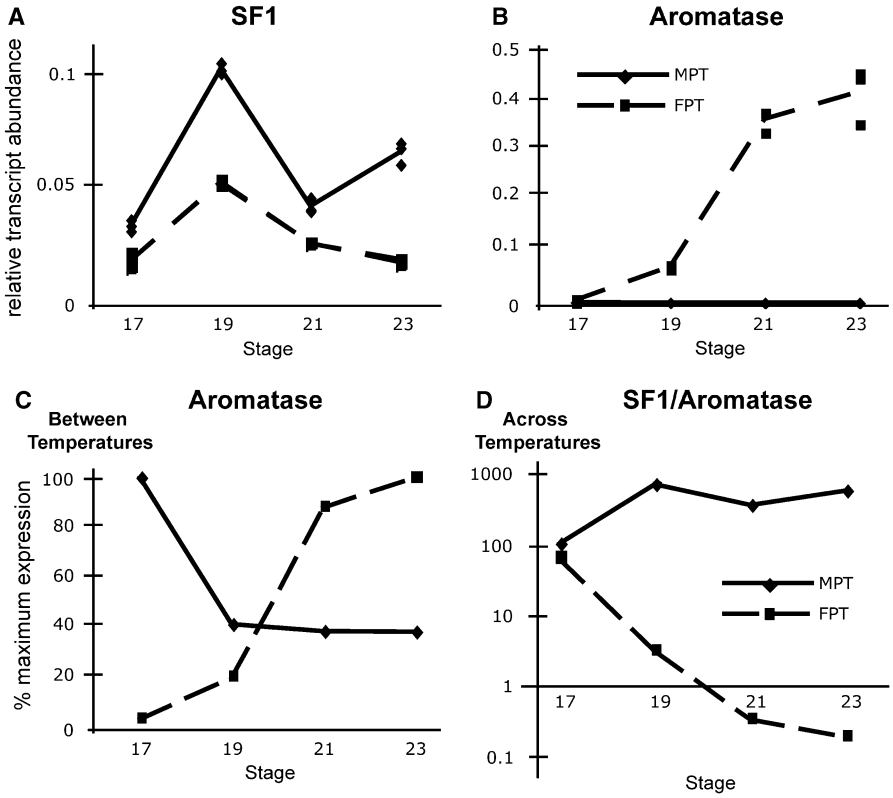

Fig. 5 Steroidogenic factor-1 (*Sf1*) gonadal transcript abundance in the gonad is higher at male-producing temperatures while aromatase is higher in putative ovaries. *Sf1* and aromatase transcript was measured by real-time quantitative PCR (qPCR). Expression of *Sf1* was higher at male-producing temperature throughout the sex-determining (Stages 17–19) and gonadal differentiation (Stages 21–23) periods of development (**A**). Expression of aromatase was equivalent between temperatures at Stage 17, but then increased in a temperature- and sex-specific manner at female-producing temperatures (**B**). Individual data points are graphed onto (A) and (B) but may not be distinct due to similarity of measurements across replicates. Late in the MPT (Stages 21, 23), aromatase was at the limit of detection for the assay, and was undetectable in two of three wells for each stage (B). Transcript abundance was measured on isolated gonad tissue from 30 to 50 pooled individuals/stage/temperature. Levels were normalized to PP1, a constitutively expressed housekeeping gene (see 'Methods'). Aromatase qPCR results were also analyzed by expressing each normalized value as % maximum of the highest level of expression for each temperature (**C**). Expression at MPT was highest (100%) at the onset of the sex-determining phase of development when the gonad is still bipotential (Stage 17), while expression at FPT was highest (100%) late in ovarian differentiation (Stage 23). The relationship between *Sf1* and aromatase qPCR results was analyzed by expressing % maximum expression across each temperature (**D**). % maximum expression was calculated across both temperatures for each gene such that all *Sf1* values were expressed relative to MPT Stage 19 (highest level of *Sf1* expression = 100%) and all aromatase values were expressed relative to FPT Stage 23 (highest level of aromatase expression = 100%). These relative values were then expressed as the ratio (*Sf1*/aromatase). MPT, male-producing temperature (26°C); FPT, female-producing temperature (31°C).

development—and the production of aromatase—varies across amniotes, and *Sf1* expression patterns vary accordingly. In mice, *Sf1* expression is down-regulated (Ikeda et al., 1994), and aromatase is not expressed during early ovarian differentiation (Greco and Payne, 1994). However, *Sf1* expression is maintained at high levels in species that do require estrogen production during ovarian differentiation such as sheep (Quirke et al., 2001), chickens (Smith et al., 1999a), and alligators (Western et al., 2000). In the current study (Fig. 5), qPCR results show higher *Sf1* expression at male- than female-producing temperatures throughout gonadal development, results consistent with previous slider turtle reports using semi-quantitative ISH analysis of gonadal expression (Fleming et al., 1999).

Sf1 is present in the undifferentiated gonad at both male- and female-producing temperatures, and a regulatory relationship between *Sf1* and aromatase cannot be excluded. *Sf1* could regulate the onset of aromatase expression at the female-producing temperature, while other factors, including a positive feedback relationship with estrogen itself, could be responsible for increasing and then maintaining high aromatase levels. In this model, temperature-specific factors would also inhibit *Sf1* up-regulation of aromatase at the male-producing temperature. However, our qPCR results indicate differential patterns in abundance between *Sf1* and aromatase. *Sf1* and aromatase also exhibit sexually dimorphic patterns of specificity/organization of expression, even at phases of gonadal development

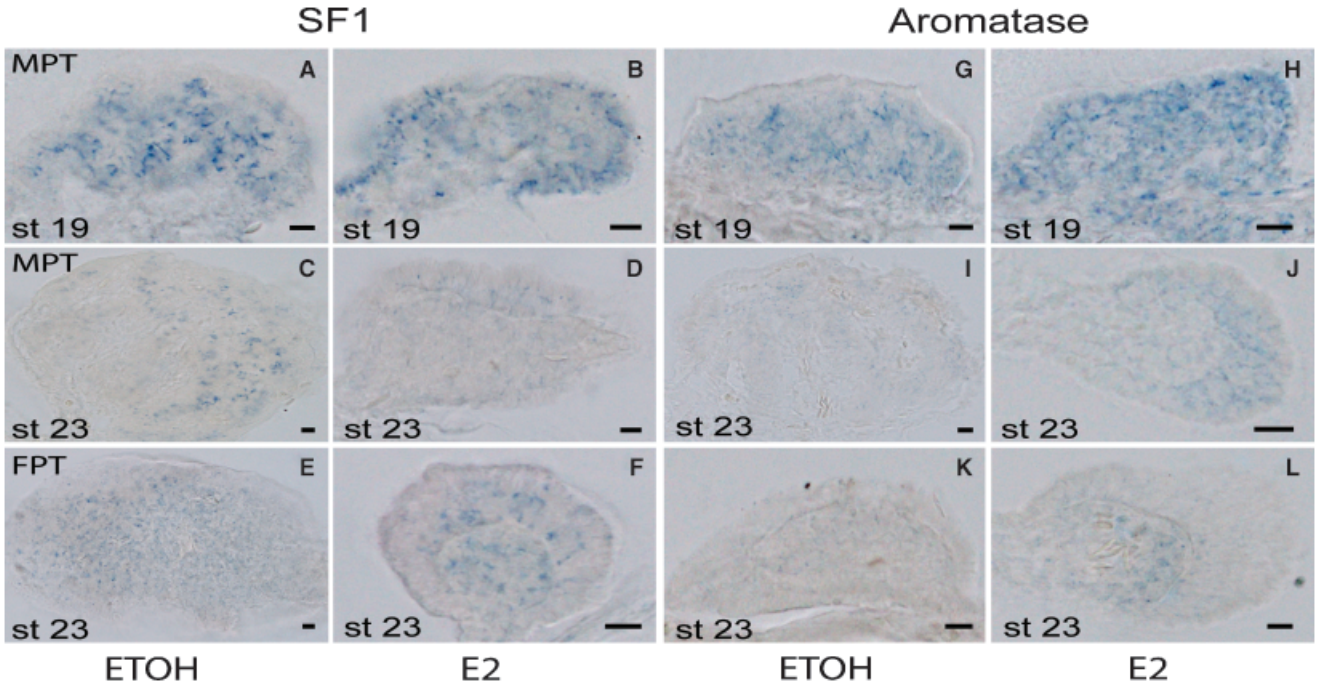

Fig. 6 Exogenous application of estradiol overcomes the male-producing temperature to produce ovaries and redirect patterns of steroidogenic factor-1 (*Sf1*) and aromatase gonadal localization while treatment at the female-producing temperature creates a unique phenotype. *Sf1* gonadal expression assumes a more diffuse, female-specific pattern of expression following application of estradiol to embryos incubating at male-producing temperatures (**A–D**). Aromatase expression is intensified following estradiol treatment, and spreads to the cortical compartment in the differentiating ovary at male-producing temperatures (**G–J**). At female-producing temperatures, estradiol application results in enlarged cortical compartments as well as altered expression patterns for *Sf1* (**E**, **F**) and aromatase (**K**, **L**). MPT, male-producing temperature (26°C); FPT, female-producing temperature (31°C). Estradiol treatment occurred at the onset of the sex-determining phase of gonadal development (Stage 17), midway through the temperature-sensitive period. Control embryos were treated with EtOH vehicle (A, C, E for *Sf1*; G, I, K for aromatase). Whole-mount gonads were sectioned at 40 μm thickness except (I, J) which were sectioned at 25 μm thickness. Scale bar = 10 μm.

when abundance is not different between the two temperatures.

Aromatase is expressed in the bipotential gonad at both temperatures, but shows an early difference in localization (Fig. 4). Aromatase is more tightly localized around putative germ cells both before and during the sex-determining phase of gonadal development at female-producing temperatures than at male-producing temperatures. The pattern is established earlier and is more widespread across the gonad at the female-producing temperature, suggesting that differential aromatase localization preceding the TSP—particularly in the supporting cell lineage surrounding germ cells in the early bipotential gonad—may set the pattern for female-specific hormone profiles affecting ovarian differentiation later in development.

In contrast, *Sf1* expression is bipotential early in development but then becomes more sex-specific and localizes around putative germ cells at the male-producing temperature during sex determination (Fig. 2). In mammals, *Sf1* is expressed in Sertoli as well as Leydig cells during testis differentiation (Ikeda et al., 1994), and its localization in the supporting cell lineage surrounding germ cells supports a conserved (non-steroidogenic?) function in slider turtle testis differentiation. The slider turtle, therefore, exhibits similarity to the mouse in terms of *Sf1* expression and testis development, but to chicken and other TSD reptile models in terms of aromatase expression and ovarian determination. This leads to the intriguing possibility that aromatase is not regulated by Sf1 in early slider turtle ovarian development. Two attractive candidates are *FoxL2* and *Lrh1*. *FoxL2* is a conserved granulosa cell marker (Schmidt et al., 2004) also expressed in developing turtle ovaries (Loffler et al., 2003; Crews et al., 2006) that regulates aromatase in goats (Pannetier et al., 2006) and chickens (Govoroun et al., 2004; Hudson et al., 2005). Another possibility is *Lrh1*, a close relative of *Sf1* that is expressed in granulosa cells and has also been shown to regulate aromatase in the mouse ovary (Hinshelwood et al., 2003).

During gonadal differentiation after the TSP has closed, *Sf1* continues to be high in the developing testis. This expression seems to localize between the sex cords later in development, and while our experiment does not allow cell type identification, it is possible this pattern reflects steroidogenic regulation within the interstitial cell lineage. It is noteworthy, however, that

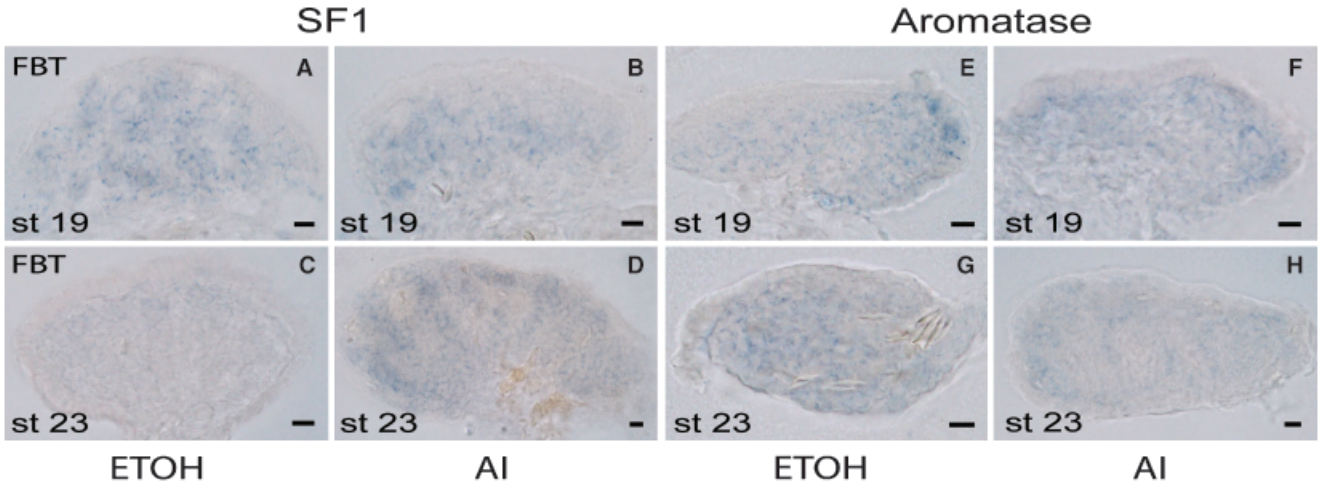

Fig. 7 Inhibition of aromatase activity overcomes the female-biased temperature to produce testes and redirect patterns of steroidogenic factor-1 (*Sf1*) and aromatase expression. *Sf1* (**A**, **B**) and aromatase (**E**, **F**) exhibit delayed response to application of aromatase inhibitor (AI) to eggs incubating at a female-biased temperature. Each gene shows sex-specific changes to AI treatment (**C**, **D** for *Sf1*; **G**, **H** for aromatase) by the time of gonadal differentiation (Stage 23). FBT, female-biased temperature (29.4°C). AI treatment occurred at the onset of the sex-determining phase of gonadal development (Stage 17), midway through the temperature-sensitive period. Control embryos were treated with EtOH vehicle (A, C for *Sf1*; E, G for aromatase). Whole-mount gonads were sectioned at 40 μm thickness. Scale bar = 10 μm.

light *Sf1* expression was detected in differentiating ovaries. This expression was observed not only throughout the medullary compartment as seen in chickens (Smith et al., 1999a) and sheep (Quirke et al., 2001), but also along the medullary/cortical boundary where steroidogenic enzymes including aromatase are expressed in fetal sheep ovaries (Quirke et al., 2001). These are the same two regions expressing aromatase in the slider turtle ovary, and may indicate Sf1 regulation of aromatase expression late in ovarian development.

During ovarian differentiation, aromatase expression as assayed by sectioned whole-mount ISH is localized primarily in the medullary compartment but the intensity of signal is faint. This low level of expression is at odds with our qPCR results. Aromatase signal is reliably detected throughout putative ovaries at earlier stages of development (Figs. 4G–I,6H,7E,7F). The reduced sensitivity of the whole-mount *in situ* method in the fully differentiated ovary (Fig. 4J) probably results from differential aromatase probe penetration into ovarian versus testis tissue at this late phase of differentiation. At the male-producing temperature, most aromatase expression is gone by the differentiation phase of testis development. However, pockets of expression localize to the interior of the seminiferous tubules, pointing to possible germ cell localization for aromatase in the differentiated testis. This expression pattern would agree with recent reports of aromatase expression in male germ cells in rats and humans (Carreau et al., 2001; Lambard et al., 2004; Lambard and Carreau, 2005).

Slider turtle sex determination is labile during the TSP, and normal gonadal development can be reversed by temperature shifts and by hormonal override of a temperature cue during the TSP (Wibbels et al., 1994). Opposing patterns of expression for *Sf1* and aromatase lead to opposite predictions during sex reversal—*Sf1* should decrease following feminizing treatment (M → F temperature shifts and estradiol treatment) and increase following masculinizing treatment (F → M temperature shifts and AI application), while aromatase should follow the opposite pattern.

Our results support these predictions. *Sf1* expression is redirected toward a diffuse female-like expression pattern following a shift from male- to female-producing temperature and exhibits the more intense, male-typical pattern following the opposing shift (Fig. 2). Given the same treatment, aromatase expression is altered toward a more organized female-typical pattern following the M → F temperature shift while expression is scattered and diffuse after the shift from F → M temperature (Fig. 4). These results affirm that (1) *Sf1* and aromatase exhibit specific sexually dimorphic patterns of expression that respond to temperature-based sex reversal, and (2) *Sf1* and aromatase localization patterns are not correlated during temperature-based sex reversal.

Our predictions are also supported when sex is reversed via the modulation of estrogen availability (Figs. 6,7). Following exogenous estradiol application during the sex-determining phase at a male-producing temperature, *Sf1* localization patterns change to a low-level female-specific pattern. In contrast, aromatase expression intensified as expected following estradiol treatment, but the localization pattern was not the same as temperature-induced ovarian differentiation. In the slider turtle, as in the chicken (Smith et al., 1999a), aromatase expression is almost exclusively medullary in the differentiating ovary (Figs. 4F,4J). The extension of

aromatase expression into the cortical compartment late in ovarian differentiation (Fig. 6J) was unique to estrogen-created ovaries. Female-producing temperatures and estrogen production are linked in the slider turtle, but their mechanism of interaction is unknown. Along with regression of the medullary sex cords, proliferation of cells in the cortical region is a major component of ovarian differentiation in the slider turtle (Wibbels et al., 1993). Continued high levels of estrogen may be required to maintain ovarian development—particularly that of the cortical compartment—in turtles maintained at male-producing temperature. In addition, our data suggest that *Sf1* expression may not be required for aromatase maintenance during estrogen-induced ovarian development at a male-producing temperature.

Temperature and estrogen have a synergistic relationship in slider turtle sex determination (Bull et al., 1990; Crews et al., 1991; Wibbels et al., 1991b), and treating embryos already incubating at a female-producing temperature with exogenous estradiol creates hyper-feminized ovaries with enlarged cortical compartments. These ''super-ovaries'' give more support to the hypothesis that estrogen plays a critical role in the proliferation of cortical cells during ovarian development, and exhibit both altered expression of *Sf1* and particularly intense aromatase expression in the medullary compartment (Figs. 6F,6L). The intense aromatase expression was surprising given that aromatase expression in the medullary region was difficult to detect in fully differentiated ovaries using whole-mount ISH. Interestingly, estrogen treatment has been shown to modulate BM and extracellular matrix (ECM) composition in the prostate gland of estrogen-treated rats (Chang et al., 1999) and up-regulate hepanarase, the enzyme that degrades hepanarase sulfate (a major polysaccharide of the BM and ECM) in MCF-7 breast cancer cells (Elkin et al., 2003). It is tempting to suggest that these estrogen-treated ovaries have modifications in the BM separating the medullary and cortical compartments of the gonad that allowed enhanced aromatase probe penetration into the interior of the ovary.

Reducing estrogen by blocking aromatase activity did not appreciably change localization patterns for either gene until late in gonadal differentiation (Fig. 7). Previous work also showed a delay in *Sf1* response to AI treatment compared with temperature shifts or estrogen application (Fleming and Crews, 2001). Presumably, this delay is due to a carry-over effect from preexisting estrogen in the gonad, as blocking aromatase activity only prevents new estrogen production.

Our results indicate that both *Sf1* and aromatase have important roles in slider turtle sex determination and differentiation. *Sf1* exhibits higher expression at male- than female-producing temperatures, indicating a conserved role in testis patterning as has been documented in mouse models. Aromatase is expressed in a female-specific manner. Both genes respond to sex-reversing treatments, but temperature and steroid treatment had different effects on sex-specific expression patterns during the sex determination phase of gonadal development. Despite its role as a regulator of steroidogenic enzymes (including aromatase), our data do not add support to the hypothesis that *Sf1* regulates female-specific aromatase expression in the developing slider turtle ovary, but do support a critical role for estrogen in ovarian development.

Acknowledgments We thank Anita Bahn and Joanna McQueen for technical assistance, Raymond Porter and James Skipper for valuable advice and support, Molly Cummings for the use of the Nikon Eclipse 80i microscope, Di Wu for taking the $\times 100$ photomicrographs, Alice Fleming for helpful comments on the manuscript, and Novartis Pharma AG, Basel, Switzerland for the gift of the CGS 16949A (Fadrazole). This work was supported by NSF grant # IBN 200001269 to D. C.

References

Baroiller, J.-F., Guiguen, Y. and Fostier, A. (1999) Endocrine and environmental aspects of sex differentiation in fish. Cell Mol Life Sci 55:910–931.

Bull, J.J., Gutzke, W.H.N. and Crews, D. (1988) Sex reversal by estradiol in three reptilian orders. Gen Comp Endocrinol 70: 425–428.

Bull, J.J., Wibbels, T. and Crews, D. (1990) Sex determining potencies vary among female incubation temperatures in a turtle. J Exp Zool 256:339–341.

Bustin, S.A. (2002) Quantification of mRNA using real-time reverse transcription PCR (RT-PCR): trends and problems. J Mol Endocrinol 29:23–39.

Carreau, S., Bourguiba, S., Lambard, S., Galeraud-Denis, I., Genissel, C., Bilinska, B., Benahmed, M. and Levallet, J. (2001) Aromatase expression in male germ cells. J Steroid Biochem Mol Biol 79:203–208.

Chang, W.Y., Wilson, M.J., Birch, L. and Prins, G. (1999) Neonatal estrogen stimulates proliferation of periductal fibroblasts and alters the extracellular matrix composition in the rat prostate. Endocrinology 140:405–415.

Coveney, D., Shaw, G. and Renfree, M.B. (2001) Estrogen-induced gonadal sex reversal in the tammar wallaby. Biol Reprod 65: 613–621.

Crews, D. and Bergeron, J.M. (1994) Role of reductase and aromatase in sex determination in the red-eared slider (*Trachemys scripta*), a turtle with temperature-dependent sex determination. J Endocrinol 143:279–289.

Crews, D., Bergeron, J.M., Bull, J.J., Flores, D., Tousignant, A., Skipper, J.K. and Wibbels, T. (1994) Temperature-dependent sex determination in reptiles: proximate mechanisms, ultimate outcomes, and practical applications. Dev Genet 15:297–312.

Crews, D., Bull, J.J. and Wibbels, T. (1991) Estrogen and sex reversal in turtles: a dose-dependent phenomenon. Gen Comp Endocrinol 81:357–364.

Crews, D., Lou, W., Fleming, A.S. and Ogawa, S. (2006) From gene networks underlying sex determination and gonadal differentiation to the development of neural networks regulating sociosexual behavior. Brain Res 1126:109–121.

Elbrecht, A. and Smith, R.G. (1992) Aromatase enzyme activity and sex determination in chickens. Science 255:467–470.

Elkin, M., Cohen, I., Zcharia, E., Orgel, A., Guatta-Rangini, Z., Peretz, T., Vlodavsky, I. and Kleinman, H.K. (2003) Regulation of heparanase gene expression by estrogen in breast cancer. Cancer Res 63:8821–8826.

Fleming, A. and Crews, D. (2001) Estradiol and incubation temperature modulate regulation of steroidogenic factor 1 in the developing gonad of the red-eared slider turtle. Endocrinology 142:1403–1411.

Fleming, A., Wibbels, T., Skipper, J.K. and Crews, D. (1999) Developmental expression of steroidogenic factor 1 in a turtle with temperature-dependent sex determination. Gen Comp Endocrinol 116:336–346.

Gabriel, W.N., Blumberg, B., Sutton, S., Place, A.R. and Lance, V.A. (2001) Alligator aromatase cDNA sequence and its expression in embryos at male and female incubation temperatures. J Exp Zool 290:439–448.

Govoroun, M., Pannetier, M., Pailhoux, E., Cocquet, J., Brillard, J.-P., Couty, I., Batellier, F. and Cotinot, C. (2004) Isolation of chicken homolog of the *FOXL2* gene and comparison of its expression patterns with those of aromatase during ovarian development. Dev Dyn 231:859–870.

Greco, T.L. and Payne, A.H. (1994) Ontogeny of expression of the genes for steroidogenic enzymes P450 side-chain cleavage, 3β-hydroxysteroid dehydrogenase, P450 17α-hydroxylase/C_{17-20} lyase, and P450 aromatase in fetal mouse gonads. Endocrinology 135:262–268.

Hinshelwood, M.M., Repa, J.J., Shelton, J.M., Richardson, J.A., Mangelsdorf, D.J. and Mendelson, C.R. (2003) Expression of LRH-1 and SF-1 in the mouse ovary: localization in different cell types correlates with differing function. Mol Cell Endocrinol 207:39–45.

Hudson, Q., Smith, C.A. and Sinclair, A.H. (2005) Aromatase inhibition reduces expression of *FOXL2* in the embryonic chicken ovary. Dev Dyn 233:1052–1055.

Ikeda, Y., Shen, W.H., Ingraham, H.A. and Parker, K.L. (1994) Developmental expression of mouse steroidogenic factor-1, and essential regulator of steroid hydroxylases. Mol Endocrinol 8:654–662.

Kettlewell, J.R., Raymond, C.S. and Zarkower, D. (2000) Temperature-dependent expression of turtle *Dmrt1* prior to sexual differentiation. Genesis 26:174–178.

Lambard, S. and Carreau, S. (2005) Aromatase and oestrogens in human male germ cells. Int J Androl 28:254–259.

Lambard, S., Galeraud-Denis, I., Saunders, P.T.K. and Carreau, S. (2004) Human immature germ cells and ejaculated spermatozoa contain aromatase and oestrogen receptors. J Mol Endocrinol 32:279–289.

Loffler, K.A., Zarkower, D. and Koopman, P. (2003) Etiology of ovarian failure in blepharophimosis ptosis epicanthus inversus syndrome: FOXL2 is a conserved, early-acting gene in vertebrate ovarian development. Endocrinology 144:3237–3243.

Maldonado, L.C.T., Piedra, A.L., Moreno-Mendoza, N., Valencia, A.M., Martinez, A.M. and Merchant-Larios, H. (2002) Expression profiles of *Dax1*, *Dmrt1*, and *Sox9* during temperature sex determination in gonads of the sea turtle *Lepidochelys olivacea*. Gen Comp Endocrinol 129:20–26.

Morohashi, K.-I. and Omura, T. (1996) Ad4BP/SF-1, a transcription factor essential for the transcription of steroidogenic cytochrome P450 genes and for the establishment of the reproductive function. FASEB J 10:1569–1577.

Murdock, C. and Wibbels, T. (2003a) Cloning and expression of aromatase in a turtle with temperature-dependent sex determination. Gen Comp Endocrinol 130:109–119.

Murdock, C. and Wibbels, T. (2003b) Expression of Dmrt in a turtle with temperature-dependent sex determination. Cytogenet Genome Res 101:302–308.

Pannetier, M., Fabre, S., Batista, F., Kocer, A., Renault, L., Jolivet, G., Mandon-Pepin, B., Cotinot, C., Veitia, R.A. and Pailhoux, E. (2006) FOXL2 activates P450 aromatase gene transcription: towards a better characterization of the early steps of mammalian ovarian development. J Mol Endocrinol 36:399–413.

Parker, K.L., Rice, D.A., Lala, D.S., Ikeda, Y., Luo, X., Wong, M., Bakke, M., Zhao, L., Frigeri, C., Hanley, N.A., Stallings, N. and Schimmer, B.P. (2002) Steroidogenic factor 1: an essential mediator of endocrine development. Recent Prog Horm Res 57:19–36.

Pfaffl, M.W. (2001) A new mathematical model for relative quantification in real-time RT-PCR. Nucleic Acids Res 29:2002–2007.

Pieau, C. and Dorizzi, M. (2004) Oestrogens and temperature-dependent sex determination in reptiles: all is in the gonads. J Endocrinol 181:367–377.

Pieau, C., Dorizzi, M. and Richard-Mercier, N. (1999) Temperature-dependent sex determination and gonadal differentiation in reptiles. Cell Mol Life Sci 55:887–900.

Quirke, L.D., Juengel, J.L., Tisdall, D.J., Lun, S., Heath, D.A. and McNatty, K.P. (2001) Ontogeny of steroidogenesis in the fetal sheep gonad. Biol Reprod 65:216–228.

Scheib, D. (1983) Effects and role of estrogens in avian gonadal differentiation. Differentiation 23:S87–S92.

Schmidt, D., Ovitt, C.E., Anlag, K., Fehsenfeld, S., Gredsted, L., Treier, A.-C. and Treier, M. (2004) The murine winged-helix transcription factor Foxl2 is required for granulosa cell differentiation and ovary maintenance. Development 131:933–942.

Simon, P. (2003) Q-Gene: processing quantitative real-time RT-PCR data. Bioinformatics 19:1439–1440.

Smith, C.A., Elf, P.K., Lang, J.W. and Joss, J.M.P. (1995) Aromatase enzyme activity during gonadal sex differentiation in alligator embryos. Differentiation 58:281–290.

Smith, C.A., Smith, M.J. and Sinclair, A.H. (1999a) Expression of chicken steroidogenic factor-1 during gonadal sex differentiation. Gen Comp Endocrinol 113:187–196.

Smith, C.A., Smith, M.J. and Sinclair, A.H. (1999b) Gene expression during gonadogenesis in the chicken embryo. Gene 234:395–402.

Spotila, L.D., Spotila, J.R. and Hall, S.E. (1998) Sequence and expression analysis of WT1 and Sox9 in the red-eared slider turtle, *Trachemys scripta*. J Exp Zool 281:417–427.

Vandesompele, J., DePreter, K.,Pattyn, F., Poppe, P., Van Roy, N., De Paepe, A. and Speleman, F. (2002) Accurate normalization of real-time quantitative RT-PCR data by geometric averaging of multiple internal control genes. Genome Biol 3:Research0034. 1-0034.11.

Wallace, H., Badawy, G.M.I. and Wallace, B.M.N. (1999) Amphibian sex determination and sex reversal. Cell Mol Life Sci 55:901–909.

Wennstrom, K. and Crews, D. (1995) Making males from females: the effects of aromatase inhibitors on a parthenogenetic species of whiptail lizard. Gen Comp Endocrinol 99:316–322.

Western, P.S., Harry, J.L., Graves, J.A.M. and Sinclair, A.H. (1999) Temperature-dependent sex determination: upregulation of SOX9 expression after commitment to male development. Dev Dyn 214:171–177.

Western, P.S., Harry, J.L., Graves, J.A.M. and Sinclair, A.H. (2000) Temperature-dependent sex determination in the American alligator: expression of *SF1*, *WT1*, and *DAX1* during gonadogenesis. Gene 241:223–232.

White, R.B. and Thomas, P. (1992) Adrenal-kidney and gonadal steroidogenesis during sexual differentiation of a reptile with temperature-dependent sex determination. Gen Comp Endocrinol 88:10–19.

Wibbels, T., Bull, J.J. and Crews, D. (1991a) Chronology and morphology of temperature-dependent sex determination. J Exp Zool 260:371–381.

Wibbels, T., Bull, J.J. and Crews, D. (1991b) Synergism between temperature and estradiol: a common pathway in turtle sex determination? J Exp Zool 260:130–134.

Wibbels, T., Bull, J.J. and Crews, D. (1994) Temperature-dependent sex determination: a mechanistic approach. J Exp Zool 270:71–78.

Wibbels, T. and Crews, D. (1994) Putative aromatase inhibitor induces male sex determination in a female unisexual lizard and in a turtle with temperature-dependent sex determination. J Endocrinol 141:295–299.

Wibbels, T., Gideon, P., Bull, J.J. and Crews, D. (1993) Estrogen- and temperature-induced medullary cord regression

during gonadal differentiation in a turtle. Differentiation 53: 149–154.

Willingham, E., Baldwin, R., Skipper, J.K. and Crews, D. (2000) Aromatase activity during embryogenesis in the brain and adrenal-kidney-gonad of the red-eared slider turtle, a species with temperature-dependent sex determination. Gen Comp Endocrinol 119:202–207.

Yntema, C.L. (1968) A series of stages in the embryonic development of *Chelydra serpentina*. J Morphol 125:219–252.